

1 **A long-term decrease in the persistence of soil carbon caused by ancient Maya land**

2 **use**

3 Peter M. J. Douglas^{1,2}, Mark Pagani¹, Timothy I. Eglinton³, Mark Brenner⁴, Jason H.

4 Curtis⁴, Andy Breckinridge⁵, Kevin Johnston⁶

5 ¹Department of Geology and Geophysics, Yale University, New Haven, CT, 06511, USA

6 ²Department of Earth and Planetary Sciences, McGill University, Montreal, QC, H3A

7 0E8, Canada

8 ³Geological Institute, ETH Zürich, Zürich, 8092, Switzerland

9 ⁴Department of Geological Sciences and Land Use and Environmental Change Institute,
10 University of Florida, Gainesville, FL, 32611, USA

11 ⁵Natural Sciences Department, University of Wisconsin–Superior, Superior, WI, 54880,
12 USA

13 ⁶Independent Scholar, Columbus, OH, 43214, USA

14

15 **Introductory Paragraph**

16 The long-term effects of deforestation on tropical forest soil carbon reservoirs are
17 poorly understood, but they are important for estimating the future consequences of
18 human land use on the global carbon cycle. The Maya Lowlands of Mexico and
19 Guatemala provide a unique opportunity to assess this question, given the widespread
20 deforestation by the ancient Maya that began ~4000 years ago. Here we present past
21 changes in the mean soil transit time of plant waxes (MTT_{wax}), determined by comparing
22 the radiocarbon ages of plant waxes and plant macrofossils, in sediment cores collected
23 from three lakes in the Maya Lowlands. Catchment-scale analyses of modern soils and

24 lake sediments indicate that MTT_{wax} reflects the age of recalcitrant carbon in deep soils.
25 All three sediment cores showed a decrease in MTT_{wax} , ranging from 600 to 2200 years,
26 from 3500 years ago to present. This decrease in MTT_{wax} , indicating reduced persistence
27 of recalcitrant carbon in lake catchment soils, is associated with palynological evidence
28 for ancient Maya deforestation. MTT_{wax} never recovered to pre-deforestation values,
29 despite a subsequent decline in human population and reforestation, implying that current
30 tropical deforestation will have long-lasting future effects on soil carbon sinks.

31

32 **Main**

33 Soil carbon is the largest terrestrial carbon reservoir (approximately 1500 Pg C)^{1,2},
34 and there is concern that it is being destabilized by climate and land use change²⁻⁴.
35 Tropical forests contain about 30% of global soil carbon stocks (~470 Pg), of which
36 about half is contained in subsoils below the organic-rich topsoil layer (typically >20-30
37 cm depth)^{1,2,5}. Radiocarbon data indicate that tropical forest subsoils contain a sizeable
38 proportion of slow-cycling carbon that persists for thousands of years⁶⁻⁸. Tropical forest
39 soil carbon is at an especially high risk of destabilization because of widespread tropical
40 deforestation over the past 50 years^{3,9}, but the impact of deforestation and land use on the
41 ability of deep soil-carbon reservoirs to store carbon over long periods of time remains
42 poorly constrained¹⁰.

43 Ancient Maya land use provides an opportunity to evaluate the long-term effects
44 of deforestation on carbon cycling in tropical forest environments. The low-elevation
45 tropical forests of southeastern Mexico and northern Central America, i.e. the Maya
46 Lowlands (Fig. 1), sustained large human populations between ca. 2500 and 1000 BP¹¹,

47 and ancient Maya urbanization and agriculture led to widespread deforestation and soil
48 erosion¹²⁻¹⁵. Furthermore, because Lowland Maya population declined substantially
49 during the Terminal Classic period (~1250 to 1100 years BP), and following the Spanish
50 conquest (~450 to 350 years BP)¹¹, the Maya Lowlands also experienced lengthy periods
51 of reduced land use intensity. Previous studies in the Maya Lowlands applied
52 palynological and sedimentological methods to infer the response of tropical forest
53 ecosystems to land use change^{12,13,15-17}, but did not evaluate changes in soil carbon
54 dynamics.

55 In this study we measured radiocarbon (¹⁴C) in long-chain (C₂₆, C₂₈, C₃₀, C₃₂) *n*-
56 alkanolic acids, which are derived from the leaf cuticular waxes of terrestrial vascular
57 plants¹⁸ (referred to here as plant waxes), in sediment cores from three lakes across the
58 Maya Lowlands (Fig. 1). Stable isotope data confirm that the plant waxes in sediments
59 from these lakes are derived from terrestrial plants^{19,20} (see Methods), and plant wax
60 production does not vary significantly among the major plant groups in these catchments,
61 angiosperm trees and grasses²¹. We define the mean transit time of plant waxes in
62 catchment soils (MTT_{wax}) as the mean age of plant waxes that are transported from soils
63 to lake sediments at a given point in time²². We calculate MTT_{wax} as the difference
64 between the age of plant waxes in sediments and the age of the sediment horizon in
65 which they were buried, which is determined by ¹⁴C analysis of plant macrofossils (see
66 Methods). Previous studies of plant-wax ¹⁴C values indicated that plant waxes are
67 representative of slow-cycling soil carbon pools in terrestrial ecosystems²³⁻²⁶, and
68 MTT_{wax} values in sediment cores thus serve as an indicator of changes in the persistence
69 of soil carbon across a catchment through time²⁷⁻²⁹.

70 *Plant-wax ^{14}C in modern catchment soils and lake sediments*

71 We compared ^{14}C measurements of plant waxes and bulk soil organic carbon
72 (SOC) in soils from the catchment of Lake Chichancanab to inform our interpretation of
73 changes in MTT_{wax} in the sediment cores. Differences in $\Delta^{14}\text{C}$ between plant waxes and
74 bulk SOC range between 9 to 51 ‰, which in subsoils (≥ 20 cm depth) corresponds to
75 ^{14}C age differences between 70 to 440 years, respectively (Fig. 2). In topsoils, age
76 differences are not easily determined because of the input of bomb-derived ^{14}C since
77 1950. Plant waxes are not consistently depleted in ^{14}C relative to bulk SOC, despite
78 typically being among the oldest and most recalcitrant fractions of soil carbon²⁶. Soils in
79 which bulk SOC is older than plant waxes may contain other refractory carbon fractions,
80 such as black carbon or petrogenic carbon³⁰. Both plant waxes and SOC in subsoil
81 horizons have negative $\Delta^{14}\text{C}$ values, indicating these carbon fractions are, on average,
82 hundreds of years old. Plant waxes in particular exhibit progressively lower $\Delta^{14}\text{C}$ in
83 deeper soils (Fig. 2). Bulk SOC $\Delta^{14}\text{C}$ exhibits a less consistent pattern with soil depth,
84 which probably reflects local-scale heterogeneity caused by processes that include the
85 input of root-derived carbon, preferential carbon flow pathways, and bioturbation³⁰. Plant
86 waxes have been found to be concentrated in mineral-bound SOC, which may account for
87 the more consistent increases in age with soil depth²⁶.

88 Plant waxes in Lake Chichancanab surface sediments are ^{14}C -depleted relative to
89 plant waxes in all catchment soil samples (Fig. 2), implying that plant waxes in the
90 sediment are largely derived from deep soils, below 50 cm²⁰. This may be a consequence
91 of subsurface transport of organic matter in this karst watersheds³¹, or to selective
92 preservation of mineral-bound plant waxes in lake sediments²⁵. These are currently the

93 only data that enable comparison of plant wax ^{14}C in soils and sediments from the same
94 catchment²⁰. Although additional datasets would help to constrain the processes that
95 control MTT_{wax} inferred from sediment cores, these results corroborate other studies that
96 indicate plant waxes are representative of mineral-associated subsoil carbon^{23,24,26}, and
97 that plant wax ages in sediments reflect the persistence of subsoil carbon in the
98 surrounding catchment^{25,32}.

99 *A long-term regional reduction in plant wax transit time*

100 Records of MTT_{wax} from the three lake cores reveal broadly consistent patterns of
101 change through time (Fig. 3A). Over the past 3500 years, a substantial decrease in
102 MTT_{wax} was recorded in all three sediment cores, with the net change in mean transit
103 time values (i.e., the difference between the highest and lowest value) ranging from
104 836 ± 300 years at Lake Chichancanab to 2290 ± 330 years at Lake Itzan.

105 The temporal pattern of the long-term decrease in MTT_{wax} differed among the
106 three lakes. At Lake Salpeten there were three distinct periods of declining MTT_{wax} :
107 during the Preclassic period (3400 to 2400 years BP), during the Classic and Postclassic
108 periods (1700 to 500 years BP), and during the past 150 years. At Salpeten there were
109 also intervals of increasing MTT_{wax} during the transition from the Preclassic to Classic
110 periods (2400 to 1700 years BP), and following the Postclassic period (500 to 150 years
111 BP). At Laguna Itzan, MTT_{wax} also declined sharply during the Preclassic period (3300 to
112 1900 years BP), but then increased gradually through the Classic and Postclassic periods
113 (1900 to 540 years BP), before declining again over the past 150 years. The record at
114 Lake Chichancanab is shorter, but indicates decreasing MTT_{wax} from the late Preclassic

115 through the Postclassic period (2200 to 650 years BP), followed by increasing MTT_{wax} to
116 the present.

117 There is a clear temporal association between deforestation, as indicated by
118 regional pollen records (Figure 3E), and declining MTT_{wax} in the three lake catchments.
119 The interval of pronounced decreasing MTT_{wax} during the Preclassic period at Salpeten
120 and Itzan corresponds to the initial deforestation of the Maya Lowlands. The end of the
121 Preclassic period was marked by a temporary reversal of deforestation (Fig. 3E) and
122 possibly decreasing regional population^{11,33}, coinciding with stabilizing or increasing
123 MTT_{wax} at Itzan and Salpeten. The Classic Period then brought renewed deforestation
124 (Fig. 3E) and peak human population densities^{11,33}, coinciding with decreased MTT_{wax} at
125 Salpeten and Chichancanab. Notably MTT_{wax} at Itzan was stable through the Classic
126 period, possibly a consequence of reduced land use pressures or implementation of soil
127 conservation practices within the catchment.

128 The transition from the Classic to the Postclassic period brought lower population
129 density and reforestation, processes that were enhanced by the Spanish Conquest that
130 began ca. 500 years BP^{11,34}. At Salpeten and Chichancanab, MTT_{wax} only began to
131 increase again following the Spanish Conquest. Finally, decreasing MTT_{wax} at Lake
132 Salpeten and Laguna Itzan over the past 150 years coincided with the rapid, extensive
133 20th-century deforestation of these catchments and throughout northern Guatemala³⁵. The
134 region surrounding Lake Chichancanab did not experience such recent deforestation,
135 likely explaining the absence of a recent decrease in MTT_{wax} there.

136 We also analyzed two deeper mid-Holocene horizons from a sediment core
137 collected at Lake Salpeten¹² (Fig. 3B), which yielded MTT_{wax} estimates of 1500 ± 225 and

138 1760±210 years. Although they do not provide a continuous record of MTT_{wax} change
139 prior to anthropogenic deforestation, these mid-Holocene MTT_{wax} values indicate that the
140 high values observed 3500 years ago at Salpeten and Itzan were not anomalous, and that
141 there was not a continuous, long-term decrease in MTT_{wax} through the Holocene. This
142 suggests that high MTT_{wax} values observed prior to major anthropogenic deforestation at
143 ~3500 years BP (Fig. 3A) represented steady-state conditions that had persisted for
144 thousands of years.

145 An alternative hypothesis is that late Holocene hydroclimate changes caused the
146 observed changes in MTT_{wax} , as previous work indicate that changes in precipitation can
147 alter MTT_{wax} in tropical forests²⁸. There is not, however, a consistent relationship
148 between paleohydrological records from the Maya Lowlands and MTT_{wax} (Fig. 3F). For
149 example, regional paleoclimate records indicate a trend towards wetter conditions
150 between 3000 and 2000 years BP³⁶, a time when we observed a pronounced decrease in
151 MTT_{wax} at Salpeten and Itzan. In contrast, the regional climate became drier between
152 2000 and 1000 years BP, while MTT_{wax} decreased at Salpeten and Chichancanab. This
153 inconsistent relationship implies that hydrological change was a secondary influence on
154 MTT_{wax} in the Maya Lowlands during the late Holocene.

155 *Mechanisms relating deforestation and plant wax transit time*

156 There are multiple mechanisms by which ancient Maya deforestation could have
157 caused the observed reduction in MTT_{wax} . Persistence of SOC is controlled largely by
158 protection from microbial biodegradation, either through sorption to mineral surfaces or
159 occlusion in soil aggregates^{10,30,37}. Mineral sorption of SOC onto Al- and Fe-bearing
160 minerals is typically favored in acidic soils, whereas Ca-mediated aggregate formation is

161 the dominant mode of soil carbon preservation in basic soils³⁷. Soils in the karstic Maya
162 lowlands form through the progressive weathering of the carbonate bedrock, and this
163 process entails gradual concentration of Al and Fe supplied by a combination of minor
164 autochthonous minerals and allochthonous inputs from dust and volcanic ash^{14,38}. Maya
165 deforestation disrupted bedrock weathering and greatly enhanced soil erosion^{12,14}.
166 Preserved soils that predate deforestation show higher concentrations of Al and Fe and
167 lower pH (as low as 5.8), compared with younger soils formed following Maya
168 deforestation (with pH as high as 8.4)¹⁴. This change in regional soil chemistry,
169 associated with deforestation, probably reduced the capacity for mineral sorption in soils,
170 and as pH rose to values near neutral, rates of microbial decomposition may have
171 increased³⁷. *N*-alkanoic acids are concentrated in mineral-bound organic matter²⁶, and
172 therefore reduced mineral sorption in the soils of the Maya lowlands soils would have
173 been particularly effective in reducing MTT_{wax} .

174 Disruption of soil aggregates is also associated with deforestation and farming,
175 through a variety of mechanisms that include tillage, increased soil disruption through
176 tree removal and crop harvesting, and interference with of root and fungal networks that
177 promote aggregation^{39,40}. Deforestation in the Maya Lowlands probably led to both
178 reduced mineral sorption and disruption of soil aggregates, both of which would have led
179 to a reduced persistence of soil carbon and lower MTT_{wax} , though the relative importance
180 of these two mechanisms is uncertain. A potential modern analog for the changes in soil
181 carbon storage in the Maya Lowlands is recent deforestation in the karst terrain of
182 southwest China, which has been associated with increasing soil pH⁴¹, the loss of carbon

183 from soil macroaggregates³⁹, and a pronounced loss of carbon from deep soils, below 50
184 cm⁴².

185 The transport of eroded soil and its effects on MTT_{wax} also require consideration,
186 as there is sedimentological evidence of enhanced soil erosion related to ancient Maya
187 deforestation during the Preclassic period, in both the Salpeten¹² and Itzan catchments
188 (Fig. 3D), although not at Chichancanab⁴³. As soil erosion progressed, it is possible that
189 surface transport of deep subsoil carbon, which contain old plant waxes, would lead to
190 increased MTT_{wax} values, as was inferred in previous studies^{27,28}. However, this is not
191 consistent with our results, as increased soil erosion at Salpeten and Itzan between 3500
192 and 2000 years BP (Fig. 3D) coincided with decreasing, rather than increasing MTT_{wax}
193 (Fig. 3A). Furthermore, as soil erosion increased during the Preclassic there was a net
194 decrease in the mass accumulation rate of plant waxes (MAR_{wax} ; Fig. 3C; see Methods)
195 at Salpeten, inconsistent with an increasing erosive input of plant waxes to the lake
196 sediments. At Itzan, MAR_{wax} first increased along with soil erosion between 3300 and
197 2600 years BP, but then MAR_{wax} decreased to its lowest levels, whereas soil erosion
198 remained at high levels between 2600 and 1900 years BP. In general, there is an
199 inconsistent relationship between MAR_{wax} and MTT_{wax} in the three lake cores, suggesting
200 that erosive transport of plant waxes was probably not a primary control on the long-term
201 decrease in MTT_{wax} .

202 Soil erosion can in some cases enhance the persistence of soil carbon by burying
203 older soils under freshly eroded material⁴⁴. However, the depositional burial of older
204 soils, which could have potentially isolated plant waxes in older carbon reservoirs and
205 prevented their transport to lake sediments, is unlikely to have caused the observed

206 decrease in MTT_{wax} . The Salpeten and Itzan catchments are small and possess relatively
207 steep slopes²⁰, and do not contain significant areas for eroded soils to accumulate aside
208 from the lakes¹². Furthermore, our comparison of modern sediments and soils at Lake
209 Chichancanab indicated that while MTT_{wax} in modern sediments is relatively low
210 compared to peak values in deeper sediments, plant wax ¹⁴C ages in modern sediments
211 are older than those found in any soil samples (Figure 2). This suggests there is not a
212 reservoir of old plant waxes in soils that is isolated from the flux transported to the lake
213 sediments.

214 *Implications for past and future soil carbon dynamics*

215 Estimates of pre-industrial land use effects on soil carbon storage are poorly
216 constrained⁴⁵, in large part because existing soil carbon models do not include long-term
217 responses of soil carbon pools to environmental change¹⁰. Comparison of the minimum
218 and maximum MTT_{wax} values calculated for each of our lake sediment cores suggests
219 that Maya deforestation reduced the transit time of plant waxes, and likely other mineral-
220 associated subsoil carbon, by between 70% (Chichancanab) to 90% (Salpeten and Itzan)
221 relative to pre-deforestation values. This implies that Maya land use strongly reduced the
222 ability of regional soils to act as long-term carbon sinks.

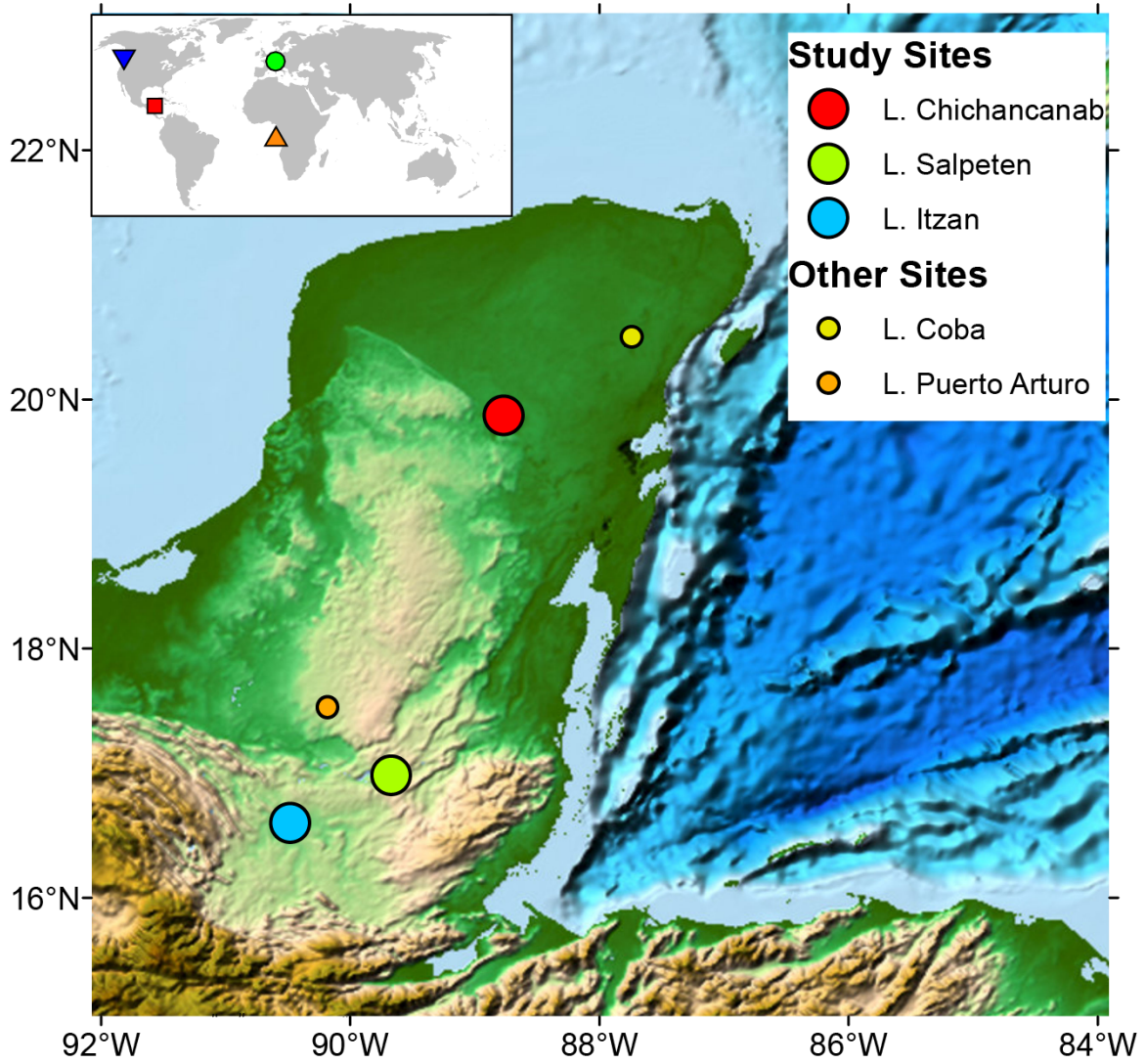
223 Comparison of our data with sediment core plant-wax ¹⁴C data from Saanich
224 Inlet, British Columbia²⁹, Lake Soppensee in Switzerland²⁷, and the Congo River Fan²⁸
225 (Fig. 4) indicates substantial geographic and temporal variability in MTT_{wax} over the past
226 ~6000 years. Detailed comparison of these records is difficult given the large differences
227 in area, climate, geology, and geomorphology of the sedimentary catchments. There is
228 clearly substantial temporal variability in MTT_{wax} in all of these records, however, with

229 values varying by more than 2000 years. This geographically widespread temporal
230 variability in MTT_{wax} suggests that the persistence of slow-cycling soil carbon has been
231 highly dynamic on millennial time-scales during the Holocene, particularly during the
232 past ~6000 years. This dynamism in soil carbon reservoirs should be validated in other
233 environments and could be important for models of Holocene carbon cycling^{45,46}. Data
234 from the Maya Lowlands and Switzerland, in particular, indicate that pre-industrial
235 human land use profoundly changed soil carbon reservoirs, which may represent a
236 substantial proportion of the pre-industrial anthropogenic impact on the global carbon
237 cycle^{45,47}.

238 The protracted decrease in MTT_{wax} in the Maya Lowlands over the past 3500
239 years suggests that extensive modern tropical deforestation will have profound long-term
240 effects on future carbon storage in tropical forest soils. Reductions in MTT_{wax} in the
241 Maya Lowlands over the past 150 years are small compared with decreases caused by
242 ancient Maya land use (Figure 3A). The first episode of declining MTT_{wax} between ca.
243 3500 and 2500 years BP, which coincided with the initial deforestation of the Maya
244 Lowlands, may be a better analogue for the recent, ongoing deforestation of primary
245 forest in many tropical regions. In general, our data indicate that MTT_{wax} decreased
246 progressively over hundreds to thousands of years (Fig. 3A), suggesting that tropical
247 forest soil carbon reservoirs, at least in subsoils, do not reach equilibrium within a few
248 decades following deforestation⁹. Instead, our results suggest that periods of sustained
249 deforestation and agriculture lead to long-term decreases in the persistence of subsoil
250 carbon over centuries to millenia.

251 MTT_{wax} in the Maya Lowlands has never recovered to the high values that
252 preceded initial deforestation, despite lengthy periods of reforestation and soil
253 stability^{12,16} (Fig. 3). This suggests that prolonged periods of time are necessary to
254 accumulate stable, slow-cycling carbon pools in reforested tropical soils, particularly if
255 past land use changed to soil chemistry in ways that diminish mineral sorption or soil
256 aggregation^{14,37,39}. These results suggest that the effects of primary tropical forest
257 removal on soil carbon reservoirs are not offset by growth of secondary forest, at least in
258 terms of long-term carbon storage in subsoils. This, in turn, implies that to maximize
259 long-term soil carbon storage, it is more effective to conserve primary forests than to
260 reforest previously deforested areas⁴⁸.

261



262

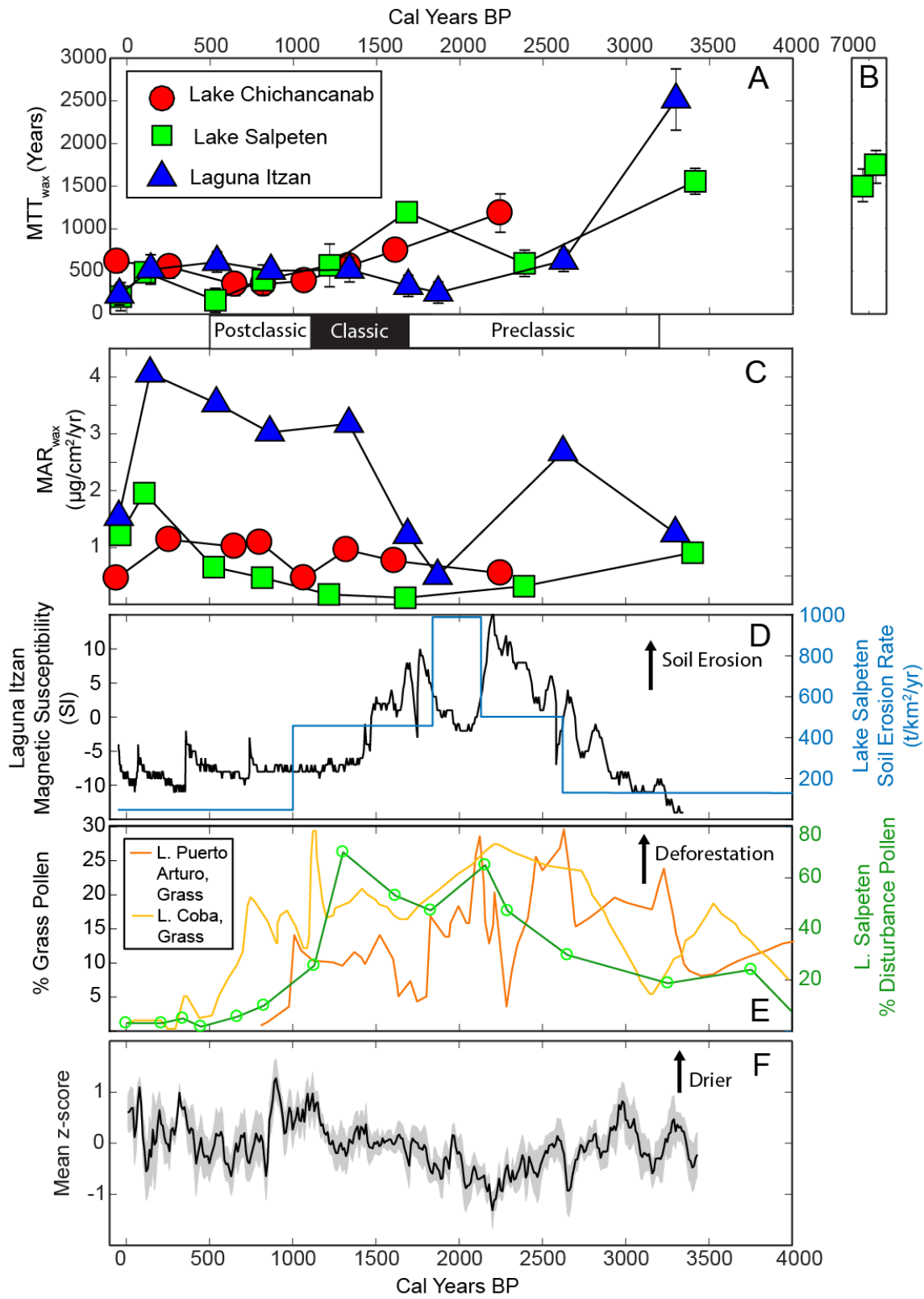
263 **Figure 1** Relief map of the Maya Lowlands indicating the location of the studied lakes.

264 Additional lakes studied for palynological records are also shown. The inset map shows the

265 location of the Maya Lowlands (red square) relative to Saanich Inlet, Canada (blue triangle), Lake

266 Soppensee, Switzerland (green circle), and the Congo River Fan (orange triangle) (see Fig. 4).

267



275

276

292 **Methods**

293 *Study Sites*

294 Lakes Chichancanab, Salpeten, and Itzan (Fig. 1) are located in representative low-
295 elevation tropical environments inhabited by the ancient Maya. All three are relatively
296 small, have limited catchments (137 to 1.5 km²)²⁰ and are located in the karst terrain that
297 characterizes most of the Maya Lowlands⁴⁹. Lakes Salpeten and Itzan contained
298 substantial ancient Maya populations within their catchments^{33,50}. For example, the
299 human population of the Lake Salpeten catchment is estimated to have peaked at around
300 4000 people during the Late Classic period, ca. 1200 BP³³. Lake Chichancanab was
301 farther from major Maya population centers and its catchment was probably less densely
302 populated⁴³, although analysis of pollen in a sediment core from the basin indicates
303 ancient maize agriculture occurred in the catchment⁵¹. Modern land use also differs
304 among the lake catchments. There has been extensive recent forest clearance in the Lake
305 Salpeten and Laguna Itzan catchments, but relatively less modern deforestation in the
306 Lake Chichancanab catchment. The lakes vary in terms of precipitation, with the greatest
307 mean annual rainfall at southernmost Laguna Itzan (2098 mm) and the least at
308 northernmost Lake Chichancanab (1161 mm)^{20,52}. This difference in rainfall is reflected
309 in the natural vegetation, with denser, higher-stature forest and a greater proportion of
310 evergreen trees in the remaining natural vegetation around Laguna Itzan and Lake
311 Salpeten, and lower-stature, more open and seasonally deciduous forest at Lake
312 Chichancanab⁵³. Soils surrounding Lake Chichancanab are primarily rendzic leptosols,
313 whereas soils in the Laguna Itzan and Lake Salpeten catchments are primarily
314 cambisols^{38,54}. Soil depths are not thoroughly mapped in the Maya Lowlands. In the

315 northern Yucatan Peninsula around Lake Chichancanab soils are typically shallow (0.5 to
316 1 m), but deeper soil profiles probably occur at the wetter sites in Guatemala^{14,38}.

317 *Sediment and soil sampling*

318 Sediment coring at Lake Chichancanab and Lake Salpeten was described
319 previously^{43,55,56}. Middle Holocene sediments from Lake Salpeten were sampled from a
320 14 m sediment core collected in 1980¹⁵, which was age-depth correlated with the cores
321 collected in 1999 from which the other samples were taken¹².

322 Two overlapping cores, totaling 5.7 m of sediment, were collected in 1997 from
323 Laguna Itzan, at a water depth of 10 m, near the western shore of the lake. The upper 2.2
324 m of sediment is dominated by silt-sized carbonate mud. Between 2.3 and 5.5 m depth
325 the sediment alternates between silt-size carbonate mud and calcite-rich clay. Magnetic
326 susceptibility of the Laguna Itzan cores was measured using a Geotek Multi-Sensor Core
327 Logger at the University of Minnesota Limnological Research Center in 1997
328 (Supplemental Table S6). Magnetic susceptibility reflects soil erosion, as it is controlled
329 by the input of magnetic, iron-bearing minerals from soils into lake sediments.

330 In all sediment cores, samples for plant-wax radiocarbon analysis were collected
331 from stratigraphic horizons as close as possible (< 2 cm), adjacent to dated terrigenous
332 macrofossils. In the Lake Salpeten and Chichancanab cores, however, we also analyzed
333 plant-wax ¹⁴C in horizons for which there were no adjacent terrigenous macrofossils to
334 distribute plant-wax ¹⁴C ages throughout the sediment cores.

335 In December 2012, soil samples were collected from sites around Lake
336 Chichancanab²⁰. Sites A and B are located in forested uplands approximately 15 and 24
337 m above lake level, respectively. Site C is near the lakeshore, < 1 meter above lake level,

338 and is inundated during periods of high water. At each site, a pit was dug and samples
339 were collected from the pit wall, with care taken to avoid contamination from overlying
340 horizons. Subsoil samples (<20 cm depth) from site C did not contain sufficient
341 quantities of long-chain fatty acids for $\Delta^{14}\text{C}_{\text{wax}}$ analysis, and were not studied further.

342 *Compound-specific radiocarbon analyses*

343 Sediment and soil samples were freeze-dried and solvent-extracted (ASE3000,
344 Dionex). Total lipid extracts were then saponified, and the acidic fraction was
345 transesterified and purified via silica gel chromatography. Purified *n*-alkanoic acids,
346 analyzed as fatty acid methyl esters (FAMES), were quantified relative to an external
347 standard using a gas chromatograph coupled to a flame ionization device. Long-chain *n*-
348 alkanolic acid methyl esters were isolated using a preparative capillary gas
349 chromatography system⁵⁷. Individual *n*-alkanoic acid homologs were not sufficiently
350 abundant for radiocarbon analyses, so we measured the combined C₂₆, C₂₈, C₃₀, and C₃₂
351 homologs. Isolated *n*-alkanoic acid samples were combusted to CO₂, graphitized, and
352 analyzed for radiocarbon at the National Ocean Sciences Accelerator Mass Spectrometry
353 (NOSAMS) Facility, Woods Hole, MA, and USA.

354 All compound-specific radiocarbon data were corrected to account for the
355 estimated procedural blank associated with sample extraction and purification⁵⁸, and they
356 also were corrected for the methyl carbon added during transesterification, which
357 contains no measurable ¹⁴C. The procedural blank determined for the WHOI Marine
358 Chemistry and Geochemistry PCGC system (which was used to isolate the Lake
359 Chichancanab samples) was 1.8±0.9 µg of C with an Fm of 0.44±10⁻⁵⁸, whereas the
360 procedural blank for the NOSAMS PCGC system (used to isolate all other samples) was

361 1.4±1.2 µg of C with an Fm of 0.64±0.2²⁰. Compound-specific radiocarbon data for
362 Lakes Salpeten and Chichancanab were previously published^{19,20}, with the exception of
363 mid-Holocene samples from Lake Salpeten (Table S1). Compound specific radiocarbon
364 data from Laguna Itzan are presented in Table S1.

365 In addition to terrestrial vascular plants, *n*-alkanoic acids can be derived from
366 aquatic plants^{59,60}, which could potentially influence the interpretations of changes in
367 MTT_{wax} presented here. Stable isotope analyses of *n*-alkanoic acids in aquatic plants from
368 the Maya Lowlands, however, indicate that they are significantly depleted in δD and δ¹³C
369 relative to plant waxes found in both regional soils in the northern Yucatan Peninsula and
370 in sediments from Lake Chichancanab and Salpeten^{19,20}. This implies that aquatic plants
371 are not an important source of plant waxes in sediments from these lakes and do not have
372 a significant effect on plant-wax ¹⁴C values. At Laguna Itzan we observed similarly
373 enriched *n*-alkanoic acid δ¹³C values in the deeper sediment samples, but more depleted
374 δ¹³C values that overlap with the range of aquatic plants in the four uppermost sediment
375 samples, from 930 years BP to present (Table S1). However, these samples postdate the
376 major decrease in MTT_{wax} in this sediment core, and therefore possible input from
377 aquatic plants in these sediment samples would not significantly alter our interpretations.
378 Furthermore, these values are also consistent with plant-wax δ¹³C values observed in
379 soils from moist tropical forest soils in southern Guatemala⁵⁹ whose climates are similar
380 to that at Laguna Itzan, as well as in plants in other low-elevation tropical forest
381 environments⁶¹. Thus the low δ¹³C values also are consistent with a dominantly terrestrial
382 plant source for long-chain *n*-alkanoic acids.

383

384 *Terrigenous macrofossil radiocarbon analyses*

385 For Lakes Chichancanab and Salpeten we compared plant-wax radiocarbon ages
386 with previously published terrigenous macrofossil radiocarbon ages^{43,55,62,63}. To establish
387 a chronology for sediment deposition at Laguna Itzan we analyzed the radiocarbon
388 content of 11 terrigenous macrofossil samples, either leaf or wood fragments, distributed
389 throughout the upper six meters of the sediment core (Supplemental Table S2). These
390 samples were pretreated using a standard acid-base-acid protocol to remove carbonate
391 minerals and humic acids⁶⁴, and they were analyzed for radiocarbon content at either the
392 Lawrence Livermore National Laboratory or DirectAMS accelerator mass spectrometry
393 laboratories.

394 *Bulk soil organic carbon isotope analyses*

395 Soil samples were sieved (2 mm) and freeze-dried, and visible plant matter was
396 removed. Samples were then homogenized and soaked in 0.5 M hydrochloric acid for 24
397 hours to remove carbonate⁶⁵, followed by repeated rinses in Milli-Q water to remove acid
398 salts. The pretreated samples were analyzed for radiocarbon content at DirectAMS
399 (Supplemental Table S3). In addition to radiocarbon analyses, we analyzed bulk soil $\delta^{13}\text{C}$
400 values using a Costech Elemental Analyzer coupled to a Thermo DeltaPlus Advantage
401 Isotope Ratio Mass Spectrometer at the Yale University Earth System Center for Stable
402 Isotope Studies (Supplemental Table S3).

403 *Sediment core age-depth models*

404 For each core, we constructed two age-depth models, one for the age of sediment
405 deposition and one for the mean age of plant-wax synthesis (Fig. S1). Sediment
406 deposition age models were based on radiocarbon ages of terrigenous plant macrofossils,

407 which is a common practice in tropical lakes in carbonate terrain, because macrofossils
408 are typically transported rapidly to sediments and their ^{14}C dates are not affected by hard-
409 water lake error^{55,62}. Plant-wax age models were based on their compound-specific
410 radiocarbon ages. For all age models, we applied the Classical Age-depth Modeling
411 (CLAM 2.1) software in R⁶⁶. All radiocarbon ages were calibrated using the IntCal13
412 calibration curve⁶⁷. 95% confidence intervals for age-depth models were calculated by
413 analyzing the distribution of 1000 randomly generated age models⁶⁶. The ‘best’ age
414 model was determined by calculating the mean age of all model iterations at each depth
415 in the core.

416 For the Lake Chichancanab and Lake Salpeten sediment cores, we applied 2nd and
417 4th order polynomial age-depth models, respectively, as applied in the original studies of
418 these cores^{43,55} (Fig. S1 A,B). The best fit to the Laguna Itzan terrigenous macrofossil
419 radiocarbon ages was provided by a 4th order polynomial age-depth model (Fig. S1 C). In
420 all cores, core-top sediments were assumed to have been deposited in the year of core
421 collection. For the middle Holocene samples from Lake Salpeten, sediment deposition
422 ages were derived from a previously published linear interpolation age model¹². To
423 develop plant-wax age-depth models at Lakes Chichancanab and Laguna Itzan we fit a
424 smoothing spline with a smoothing factor of 0.3 to the $^{14}\text{C}_{\text{wax}}$ ages (Fig. S1 A,C). At Lake
425 Salpeten the best-fit age-depth model for plant waxes was provided by linear
426 interpolation between dated horizons (Fig. S1 B).

427 The mean transit time of plant waxes in catchment soils (MTT_{wax}) was calculated
428 as the age difference, for each depth in the core, between the plant-wax and sediment
429 age-depth models. We applied the difference in the calibrated ages of the age-depth

430 models because we do not have macrofossil ^{14}C ages for all core depths where we
431 measured plant wax ^{14}C ages. MTT_{wax} represents the mean age of plant waxes at the time
432 of sediment deposition. This calculation assumes that transit times between plants and
433 catchment soils and from soils to lake sediments is rapid. This assumption is reasonable
434 given that plant waxes are derived predominantly from leaves⁶⁸, which turnover within a
435 few years⁶⁹, as well as the small catchment sizes, shallow lake water depths (10 to 32 m)
436 and absence of apparent intermediate reservoirs²⁰. MTT_{wax} confidence intervals were
437 estimated by propagating the 95% confidence intervals for the plant-wax and sediment
438 age-depth models (Fig. S1). MTT_{wax} values and the sediment and plant-wax ages used to
439 calculate them are shown in Supplemental Table S4.

440 *Calculation of plant-wax mass accumulation rates*

441 To calculate MAR_{wax} we used the general equation:

$$442 \quad \text{MAR}_{\text{wax}} = c_{\text{wax}} \times \text{SAR} \times \text{DBD} \quad (1)$$

443 where c_{wax} is the concentration of plant waxes in lake sediments ($\mu\text{g C}_{26}$, C_{28} , C_{30} ,
444 and C_{32} alkanolic acids per g dry sediment, measured using gas chromatography with a
445 flame ionization detector in comparison with an external FAME standard), SAR is the
446 sediment accumulation rate determined from the terrigenous macrofossil age-depth
447 models (Fig. S1), and DBD is the dry bulk density of core sediments (g dry sediment per
448 cm^{-3} wet sediment). Values for all of these sediment variables are shown in Supplemental
449 Table S5.

450 For the Lake Chichancanab core, wet bulk density (WBD; g wet/ cm^3 of wet
451 sediment) data were available⁴³, but we did not have data for sediment porosity or water
452 content, and so we used the following equation to estimate dry bulk density (DBD):

453 $DBD = WBD - (1.025 * 0.9)$ (Equation 1)

454 where 1.025 represents the density of saline lake waters and 0.9 is an estimate for the
455 porosity of the organic-rich gyttja sediments, based on studies from other lakes^{12,70}. An
456 assumption of constant porosity is valid at this lake, where sediment lithology varies
457 little⁴³.

458 For the Lake Salpeten core, for which WBD data were not available, we estimated
459 DBD using the following formula⁷¹:

460
$$DBD = \frac{D(2.5I + 1.6C)}{D + (1 - D)(2.5I + 1.6C)}$$
 (Eq. 2)

461 where D is the proportion of dry mass in wet sediment, I is the inorganic proportion of
462 dry material (density $\sim 2.5 \text{ g/cm}^3$), and C is the organic proportion of dry material
463 (density $\sim 1.6 \text{ g/cm}^3$). Whereas 1.6 g/cm^3 was the density of organic matter used in the
464 original application of this equation, organic matter can have lower densities.
465 Nevertheless, even using a density of 1.25 g/cm^3 produced negligible changes in our
466 calculated MAR_{wax} values. D , I , and C were determined based on water content analyses
467 and weight loss on ignition at $550 \text{ }^\circ\text{C}$ using a sediment core from Lake Salpeten collected
468 in 1980⁷², and were correlated to sediment depths in the 1999 Lake Salpeten sediment
469 cores analyzed in this study using a composite age model^{12,55}.

470 At Laguna Itzan we estimated DBD by sampling 2 cm^3 of wet sediment at 10-cm
471 intervals throughout the sediment core, drying the sediment in a 70°C oven, and
472 measuring the dry sediment mass. It was not possible to perform this procedure in the
473 uppermost meter of core sediments because of long-term drying of stored sediment cores.
474 For these horizons, we estimated dry bulk density by applying a 2nd order polynomial

475 regression between WBD (measured using a Geotek multi-sensor core logger), and DBD
476 estimates for lower core sediments described above ($R^2 = 0.75$).

477 Within-core variation in MAR_{wax} is dominantly controlled by c_{wax} , and is not
478 strongly correlated with SAR or DBD (Supplementary Table S5). Therefore we consider
479 the temporal trends within a particular record, which is our primary focus, to be robust.
480 Given the different approaches to calculating sediment density for each core, differences
481 in absolute MAR_{wax} values between the lake sediment cores should be interpreted
482 cautiously.

483 **Data Availability Statement**

484 The data that support the findings of this paper are available either as tables in the
485 supplementary information file or in tables published in the peer-reviewed articles cited
486 in the Methods. All data are available in a spreadsheet format upon request from the
487 corresponding author.

488
489
490

491 **References**

492

- 493 1 Hiederer, R. & Köchy, M. Global soil organic carbon estimates and the
494 harmonized world soil database. . 79 pp. (Publications Office of the European
495 Union, 2011).
- 496 2 Scharlemann, J. P., Tanner, E. V., Hiederer, R. & Kapos, V. Global soil carbon:
497 understanding and managing the largest terrestrial carbon pool. *Carbon*
498 *Management* **5**, 81-91 (2014).
- 499 3 Moore, S. *et al.* Deep instability of deforested tropical peatlands revealed by
500 fluvial organic carbon fluxes. *Nature* **493**, 660-663 (2013).
- 501 4 Conant, R. T. *et al.* Temperature and soil organic matter decomposition rates–
502 synthesis of current knowledge and a way forward. *Global Change Biol* **17**, 3392-
503 3404 (2011).
- 504 5 Jobbagy, E. G. & Jackson, R. B. The vertical distribution of soil organic carbon
505 and its relation to climate and vegetation. *Ecol Appl* **10**, 423-436 (2000).
- 506 6 Torn, M. S., Trumbore, S. E., Chadwick, O. A., Vitousek, P. M. & Hendricks, D.
507 M. Mineral control of soil organic carbon storage and turnover. *Nature* **389**, 170-
508 173 (1997).
- 509 7 He, Y. *et al.* Radiocarbon constraints imply reduced carbon uptake by soils during
510 the 21st century. *Science* **353**, 1419-1424 (2016).
- 511 8 Trumbore, S. Age of soil organic matter and soil respiration: Radiocarbon
512 constraints on belowground C dynamics. *Ecol Appl* **10**, 399-411 (2000).

- 513 9 Don, A., Schumacher, J. & Freibauer, A. Impact of tropical land-use change on
514 soil organic carbon stocks: a meta-analysis. *Global Change Biol* **17**, 1658-1670
515 (2011).
- 516 10 Schmidt, M. W. I. *et al.* Persistence of soil organic matter as an ecosystem
517 property. *Nature* **478**, 49-56 (2011).
- 518 11 Turner II, B. L. in *Precolumbian Population History in the Maya Lowlands* (eds
519 T. P. Culbert & D. S. Rice) 301-324 (University of New Mexico Press, 1990).
- 520 12 Anselmetti, F. S., Hodell, D. A., Ariztegui, D., Brenner, M. & Rosenmeier, M. F.
521 Quantification of soil erosion rates related to ancient Maya deforestation. *Geology*
522 **35**, 915-918 (2007).
- 523 13 Wahl, D., Byrne, R., Schreiner, T. & Hansen, R. Palaeolimnological evidence of
524 late-Holocene settlement and abandonment in the Mirador Basin, Peten,
525 Guatemala. *Holocene* **17**, 813-820 (2007).
- 526 14 Beach, T. *et al.* Stability and instability on Maya Lowlands tropical hillslope soils.
527 *Geomorphology* **305**, 185-208 (2018).
- 528 15 Leyden, B. W. Man and Climate in the Maya Lowlands. *Quaternary Res* **28**, 407-
529 417 (1987).
- 530 16 Mueller, A. D. *et al.* Recovery of the forest ecosystem in the tropical lowlands of
531 northern Guatemala after disintegration of Classic Maya polities. *Geology* **38**,
532 523-526 (2010).
- 533 17 Leyden, B. W., Brenner, M. & Dahlin, B. H. Cultural and climatic history of
534 Coba, a lowland Maya city in Quintana Roo, Mexico. *Quaternary Res* **49**, 111-
535 122 (1998).
- 536 18 Kolattukudy, P. Plant waxes. *Lipids* **5**, 259-275 (1970).
- 537 19 Douglas, P. M. *et al.* Drought, agricultural adaptation, and sociopolitical collapse
538 in the Maya Lowlands. *Proceedings of the National Academy of Sciences* **112**,
539 5607-5612 (2015).
- 540 20 Douglas, P. M. *et al.* Pre-aged plant waxes in tropical lake sediments and their
541 influence on the chronology of molecular paleoclimate proxy records. *Geochim*
542 *Cosmochim Ac* **141**, 346-364 (2014).
- 543 21 Bush, R. T. & McInerney, F. A. Leaf wax *n*-alkane distributions in and across
544 modern plants: Implications for paleoecology and chemotaxonomy. *Geochim*
545 *Cosmochim Ac* **117**, 161-179 (2013).
- 546 22 Sierra, C. A., Müller, M., Metzler, H., Manzoni, S. & Trumbore, S. E. The
547 middle of ages, turnover, transit, and residence times in the carbon cycle. *Global*
548 *Change Biol* **23**, 1763-1773 (2017).
- 549 23 Tao, S., Eglinton, T. I., Montluçon, D. B., McIntyre, C. & Zhao, M. Pre-aged soil
550 organic carbon as a major component of the Yellow River suspended load:
551 Regional significance and global relevance. *Earth Planet Sc Lett* **414**, 77-86
552 (2015).
- 553 24 Feng, X. *et al.* Differential mobilization of terrestrial carbon pools in Eurasian
554 Arctic river basins. *Proceedings of the National Academy of Sciences* **110**, 14168-
555 14173 (2013).
- 556 25 Vonk, J. E., van Dongen, B. E. & Gustafsson, O. Selective preservation of old
557 organic carbon fluvially released from sub-Arctic soils. *Geophys Res Lett* **37**, -
558 (2010).

- 559 26 Voort, T. *et al.* Diverse soil carbon dynamics expressed at the molecular level.
560 *Geophys Res Lett* **44**, 11840-11850 (2017).
- 561 27 Gierga, M. *et al.* Long-stored soil carbon released by prehistoric land use:
562 Evidence from compound-specific radiocarbon analysis on Soppensee lake
563 sediments. *Quaternary Sci Rev* **144**, 123-131 (2016).
- 564 28 Schefuß, E. *et al.* Hydrologic control of carbon cycling and aged carbon discharge
565 in the Congo River basin. *Nat Geosci* **9**, 687-690 (2016).
- 566 29 Smittenberg, R. H., Eglinton, T. I., Schouten, S. & Damste, J. S. S. Ongoing
567 buildup of refractory organic carbon in boreal soils during the Holocene. *Science*
568 **314**, 1283-1286 (2006).
- 569 30 Rumpel, C. & Kögel-Knabner, I. Deep soil organic matter—a key but poorly
570 understood component of terrestrial C cycle. *Plant Soil* **338**, 143-158 (2011).
- 571 31 Lechleitner, F. A., Dittmar, T., Baldini, J. U., Prufer, K. M. & Eglinton, T. I.
572 Molecular signatures of dissolved organic matter in a tropical karst system. *Org*
573 *Geochem* **113**, 141-149 (2017).
- 574 32 Drenzek, N. J., Montlucon, D. B., Yunker, M. B., Macdonald, R. W. & Eglinton,
575 T. I. Constraints on the origin of sedimentary organic carbon in the Beaufort Sea
576 from coupled molecular C-13 and C-14 measurements. *Mar Chem* **103**, 146-162
577 (2007).
- 578 33 Rice, D. & Rice, P. in *Precolumbian Population History in the Maya Lowlands*
579 (eds TP Culbert & DS Rice) 123-148 (University of New Mexico Press, 1990).
- 580 34 Dunning, N. P. & Beach, T. in *Landscapes and Societies: Selected Cases* (eds I.
581 P. Martini & Ward Chesworth) 369-389 (Springer, 2011).
- 582 35 Schwartz, N. in *The Social Causes of Deforestation in Latin America* (eds N
583 Schwartz, M Painter, & WH Durham) 101-130 (University of Michigan Press,
584 1995).
- 585 36 Douglas, P. M., Demarest, A. A., Brenner, M. & Canuto, M. A. Impacts of
586 climate change on the collapse of Lowland Maya civilization. *Annual Review of*
587 *Earth and Planetary Sciences* **44**, 613-645 (2016).
- 588 37 Rowley, M. C., Grand, S. & Verrecchia, É. P. Calcium-mediated stabilisation of
589 soil organic carbon. *Biogeochemistry* **137**, 27-49 (2018).
- 590 38 Bautista, F., Palacio-Aponte, G., Quintana, P. & Zinck, J. A. Spatial distribution
591 and development of soils in tropical karst areas from the Peninsula of Yucatan,
592 Mexico. *Geomorphology* **135**, 308-321 (2011).
- 593 39 Xiao, S., Zhang, W., Ye, Y., Zhao, J. & Wang, K. Soil aggregate mediates the
594 impacts of land uses on organic carbon, total nitrogen, and microbial activity in a
595 Karst ecosystem. *Scientific Reports* **7**, 41402 (2017).
- 596 40 Six, J., Conant, R., Paul, E. A. & Paustian, K. Stabilization mechanisms of soil
597 organic matter: implications for C-saturation of soils. *Plant Soil* **241**, 155-176
598 (2002).
- 599 41 Jiang, Y.-J. *et al.* Impact of land-use change on soil properties in a typical karst
600 agricultural region of Southwest China: a case study of Xiaojiang watershed,
601 Yunnan. *Environmental Geology* **50**, 911 (2006).
- 602 42 Hu, Y., Du, Z., Wang, Q. & Li, G. Combined deep sampling and mass-based
603 approaches to assess soil carbon and nitrogen losses due to land-use changes in
604 karst area of southwestern China. *Solid Earth* **7**, 1075-1084 (2016).

605 43 Hodell, D. A., Brenner, M. & Curtis, J. H. Terminal Classic drought in the
606 northern Maya lowlands inferred from multiple sediment cores in Lake
607 Chichancanab (Mexico). *Quaternary Sci Rev* **24**, 1413-1427 (2005).

608 44 Berhe, A. A. & Kleber, M. Erosion, deposition, and the persistence of soil organic
609 matter: mechanistic considerations and problems with terminology. *Earth Surf
610 Proc Land* **38**, 908-912 (2013).

611 45 Kaplan, J. O. *et al.* Holocene carbon emissions as a result of anthropogenic land
612 cover change. *Holocene* **21**, 775-791 (2011).

613 46 Bauska, T. K. *et al.* Links between atmospheric carbon dioxide, the land carbon
614 reservoir and climate over the past millennium. *Nat Geosci* **8**, 383-387 (2015).

615 47 Ruddiman, W. F. The anthropogenic greenhouse era began thousands of years
616 ago. *Climatic Change* **61**, 261-293 (2003).

617 48 Luysaert, S. *et al.* Old-growth forests as global carbon sinks. *Nature* **455**, 213-
618 215 (2008).

619 49 Bauer-Gottwein, P. *et al.* Review: The Yucatán Peninsula karst aquifer, Mexico.
620 *Hydrogeology Journal* **19**, 507-524 (2011).

621 50 Johnston, K. J. Preclassic Maya occupation of the Itzan escarpment, lower Río de
622 la Pasión, Petén, Guatemala. *Ancient Mesoamerica* **17**, 177-201 (2006).

623 51 Leyden, B. W. Pollen evidence for climatic variability and cultural disturbance in
624 the Maya lowlands. *Ancient Mesoamerica* **13**, 85-101 (2002).

625 52 New, M., Lister, D., Hulme, M. & Makin, I. A high-resolution data set of surface
626 climate over global land areas. *Climate Research* **21**, 1-25 (2002).

627 53 Olson, D. M. *et al.* Terrestrial ecoregions of the world: A new global map of
628 terrestrial ecoregions provides an innovative tool for conserving biodiversity.
629 *BioScience* **51**, 933-938 (2001).

630 54 Nachtergaele, F. *et al.* Harmonized world soil database version 1.1.
631 (FAO/IIASA/ISRIC/ISS-CAS, Rome, Italy and Laxenberg, Austria, 2009).

632 55 Rosenmeier, M. F., Hodell, D. A., Brenner, M., Curtis, J. H. & Guilderson, T. P.
633 A 4000-year lacustrine record of environmental change in the southern Maya
634 lowlands, Peten, Guatemala. *Quaternary Res* **57**, 183-190 (2002).

635 56 Rosenmeier, M. F. *et al.* Influence of vegetation change on watershed hydrology:
636 implications for paleoclimatic interpretation of lacustrine $\delta^{18}\text{O}$ records. *J
637 Paleolimnol* **27**, 117-131 (2002).

638 57 Eglinton, T. I., Aluwihare, L. I., Bauer, J. E., Druffel, E. R. M. & McNichol, A. P.
639 Gas chromatographic isolation of individual compounds from complex matrices
640 for radiocarbon dating. *Analytical Chemistry* **68**, 904-912 (1996).

641 58 Galy, V. & Eglinton, T. Protracted storage of biospheric carbon in the Ganges-
642 Brahmaputra basin. *Nat Geosci* **4**, 843-847 (2011).

643 59 Douglas, P. M. J., Pagani, M., Brenner, M., Hodell, D. A. & Curtis, J. H. Aridity
644 and vegetation composition are important determinants of leaf-wax δD values in
645 southeastern Mexico and Central America. *Geochim Cosmochim Acta* **97**, 24-45
646 (2012).

647 60 Liu, H. & Liu, W. Concentration and distributions of fatty acids in algae,
648 submerged plants and terrestrial plants from the northeastern Tibetan Plateau. *Org
649 Geochem* **113**, 17-26 (2017).

- 650 61 Wu, M. S. *et al.* Altitude effect on leaf wax carbon isotopic composition in humid
651 tropical forests. *Geochim Cosmochim Acta* **206**, 1-17 (2017).
- 652 62 Hodell, D. A., Curtis, J. H. & Brenner, M. Possible Role of Climate in the
653 Collapse of Classic Maya Civilization. *Nature* **375**, 391-394 (1995).
- 654 63 Hodell, D. A., Brenner, M., Curtis, J. H. & Guilderson, T. Solar forcing of
655 drought frequency in the Maya lowlands. *Science* **292**, 1367-1370 (2001).
- 656 64 Brock, F., Higham, T., Ditchfield, P. & Ramsey, C. B. Current pretreatment
657 methods for AMS radiocarbon dating at the Oxford Radiocarbon Accelerator Unit
658 (ORAU). *Radiocarbon* **52**, 103-112 (2010).
- 659 65 Midwood, A. & Boutton, T. Soil carbonate decomposition by acid has little effect
660 on $\delta^{13}\text{C}$ of organic matter. *Soil Biology and Biochemistry* **30**, 1301-1307 (1998).
- 661 66 Blaauw, M. Methods and code for 'classical' age-modelling of radiocarbon
662 sequences. *Quat Geochronol* **5**, 512-518 (2010).
- 663 67 Reimer, P. J. *et al.* IntCal13 and Marine13 radiocarbon age calibration curves 0–
664 50,000 years cal BP. *Radiocarbon* **55**, 1869-1887 (2013).
- 665 68 Häggi, C., Zech, R., McIntyre, C. & Eglinton, T. On the stratigraphic integrity of
666 leaf-wax biomarkers in loess-paleosols. *Biogeosciences* **11**, 2455-2463 (2014).
- 667 69 Hikosaka, K. Leaf canopy as a dynamic system: ecophysiology and optimality in
668 leaf turnover. *Annals of Botany* **95**, 521-533 (2004).
- 669 70 Cornett, R., Risto, B. & Lee, D. Measuring groundwater transport through lake
670 sediments by advection and diffusion. *Water Resources Research* **25**, 1815-1823
671 (1989).
- 672 71 Binford, M. W. Calculation and uncertainty analysis of ^{210}Pb dates for PIRLA
673 project lake sediment cores. *J Paleolimnol* **3**, 253-267 (1990).
- 674 72 Deevey Jr, E. S., Brenner, M. & Binford, M. W. Paleolimnology of the Peten
675 Lake District, Guatemala III: Late Pleistocene and Gamblian environments of the
676 Maya area. *Hydrobiologia* **103**, 211-216 (1983).
- 677

678

679 **Corresponding Author:**

680 Correspondence to Peter Douglas (peter.douglas@mcgill.ca).

681

682 **Acknowledgments:** This paper is dedicated to Mark Pagani. Thanks to Ann McNichol
683 and Li Xu for facilitating the compound specific radiocarbon measurements. Funding for
684 this work was provided, in part, by a U.S. National Science Foundation Graduate
685 Research Fellowship (to PMJD) and by a grant from the Italian Ministry of the
686 Environment (to MP).

687 **Author Contribution Statement:** PMJD and MP designed the study; MB, JAH, AB,
688 and KJ collected, described, and sampled the sediment cores; PMJD performed the
689 geochemical analyses, under the guidance of TIE and MP; PMJD analyzed the data and
690 wrote the manuscript, with input from all authors.

691

692

693

694

695

696

697